

# INTEGRATED LAYERED MANUFACTURING OF A NOVEL WIRELESS MOTION SENSOR SYSTEM WITH GPS

Misael Navarrete, Amit Lopes, Jacqueline Acuna, Raul Estrada, Eric MacDonald,  
Jeremy Palmer\*, and Ryan Wicker  
The University of Texas at El Paso, W.M. Keck Center for 3D Innovation,  
El Paso, Texas 79968

\*Sandia National Laboratories  
Albuquerque, New Mexico 87185-0958

Reviewed, accepted August 31, 2007

## Abstract

A programmable wireless motion sensor system with Global Positioning System (GPS) navigation capabilities was designed and manufactured for border security applications. The sensor was freeform manufactured using a previously developed layered manufacturing (LM) system that combines direct write (DW) conductive ink dispensing with stereolithography (SL). Electronic components were selected based on constraints imposed through the LM process and components included a low power rPIC12F675K microcontroller with integrated radio frequency transmitter circuitry, Panasonic passive infrared motion sensor, and a Polstar GPS module. This circuit was selected to expand on the previously described capabilities of the hybrid SL/DW setup to fabricate three-dimensional (3D) circuits, and the circuit was designed for LM to include a real wireless application, fewer external components, low voltage requirements, and simplicity to program the microcontroller. LM benefited the design and manufacturing of the sensor in comparison to traditional PCB manufacturing by (1) reducing the overall size of the sensor due to the 3D locations of components and circuitry, (2) allowing the overall shape of the sensor to change according to the environment in which it will be placed (so that it can take on the form of the local terrain, for example), and (3) providing a natural resistance to reverse engineering through 3D circuitry and component embedding.

*Keywords: rapid prototyping; stereolithography; direct-write; hybrid integrated manufacturing; wireless sensor*

## Introduction

Distributed ground networks offer a potential solution to provide monitoring of multiple conditions such as motion, audio, ground vibrations and chemical/gas detection in large remote areas and under extreme environments. Due to their ability to process large amounts of data, unattended sensors have potential applications for US border security, industrial automation and real-time monitoring. This paper proposes a border security application which can enable manpower to be used efficiently, reduce overall surveillance costs, and increase overall productivity of the security force while greatly assisting border security efforts. The functional requirements desired for this type of application include:

- resistant to reverse engineering
- difficult to detect by violators
- durable
- capable of operating in extreme (high) temperatures
- mobile
- self-locating

Report Documentation Page				Form Approved OMB No. 0704-0188	
Public reporting burden for the collection of information is estimated to average 1 hour per response, including the time for reviewing instructions, searching existing data sources, gathering and maintaining the data needed, and completing and reviewing the collection of information. Send comments regarding this burden estimate or any other aspect of this collection of information, including suggestions for reducing this burden, to Washington Headquarters Services, Directorate for Information Operations and Reports, 1215 Jefferson Davis Highway, Suite 1204, Arlington VA 22202-4302. Respondents should be aware that notwithstanding any other provision of law, no person shall be subject to a penalty for failing to comply with a collection of information if it does not display a currently valid OMB control number.					
1. REPORT DATE <b>AUG 2007</b>		2. REPORT TYPE		3. DATES COVERED <b>00-00-2007 to 00-00-2007</b>	
4. TITLE AND SUBTITLE <b>Integrated Layered Manufacturing Of A Novel Wireless Motion Sensor System With GPS</b>				5a. CONTRACT NUMBER	
				5b. GRANT NUMBER	
				5c. PROGRAM ELEMENT NUMBER	
6. AUTHOR(S)				5d. PROJECT NUMBER	
				5e. TASK NUMBER	
				5f. WORK UNIT NUMBER	
7. PERFORMING ORGANIZATION NAME(S) AND ADDRESS(ES) <b>The University of Texas at El Paso,W.M. Keck Center for 3D Innovation, ,El Paso,TX,79968</b>				8. PERFORMING ORGANIZATION REPORT NUMBER	
9. SPONSORING/MONITORING AGENCY NAME(S) AND ADDRESS(ES)				10. SPONSOR/MONITOR'S ACRONYM(S)	
				11. SPONSOR/MONITOR'S REPORT NUMBER(S)	
12. DISTRIBUTION/AVAILABILITY STATEMENT <b>Approved for public release; distribution unlimited</b>					
13. SUPPLEMENTARY NOTES <b>See also ADM002161. Presented at Symposium on Solid Freeform Fabrication (SFF)(18th) held in Austin, TX on 6-8 August 2007. Published in Proceedings on Solid Freeform Fabrication (SFF) (18th), pvii-ix, 1-609, 2007. U.S. Government or Federal Rights License.</b>					
14. ABSTRACT <b>See Report.</b>					
15. SUBJECT TERMS					
16. SECURITY CLASSIFICATION OF:			17. LIMITATION OF ABSTRACT <b>Same as Report (SAR)</b>	18. NUMBER OF PAGES <b>11</b>	19a. NAME OF RESPONSIBLE PERSON
a. REPORT <b>unclassified</b>	b. ABSTRACT <b>unclassified</b>	c. THIS PAGE <b>unclassified</b>			

To meet these functional requirements, a wireless motion sensor with navigation capabilities via an onboard GPS receiver that communicates sensor activity and GPS data over an unregulated radio frequency (RF) transmission in an arbitrarily, 3D manufactured package is proposed. Recent advances in Rapid Prototyping of High Density Circuitry (RPHDC) research and, specifically, the development of a hybrid stereolithography and direct-write system (SL/DW) have enabled the fabrication of 3D structures with high-resolution electrically conductive media (Medina *et al.*, 2005a and b). Stereolithography (SL) is one of the most widely used RP technologies to manufacture highly complex and accurate 3D prototypes due to its high build resolution. The use of different materials and the ability to build in arbitrary geometries can enable the design and manufacture of compact and visually appealing 3D circuits. Fabricating in several structured functional layers can reduce the overall circuit size and embedding the electronic components within the design can provide enhanced protection from harsh environments while increasing the overall strength and reliability of the final product (Lopes *et al.*, 2006).

We have previously described a semi-automatic hybrid SL/DW manufacturing setup to enable research in these areas (Medina *et al.*, 2005a and b; Lopes *et al.*, 2006). In this integrated manufacturing environment, SL is employed in conjunction with DW fluid dispensing technology to capitalize on each of the individual process capabilities for developing advanced electromechanical devices. Previous research determined that the DSM Somos® ProtoTherm™ 12120 resin (DSM Somos®, New Castle Delaware) provided the best resin alternative for the SL build due to its high heat deflection, relatively low viscosity, and its ability to build without sweeping (Lopes *et al.*, 2006). The E1660 silver conductive ink (E1660-136, Ercon, Wareham, MA) was also shown to provide superior characteristics for the SL/DW application; it was initially selected due to its low curing temperature (138°C for 10 minutes), and its low resistivity (Lopes *et al.*, 2006).

Using the SL/DW system, we successfully fabricated a fully functional LM555 temperature sensor circuit with embedded passive electrical components and DW interconnections between components as shown in Figure 1 (Lopes *et al.*, 2006). The 555 timer circuit is based on the sequential charging and discharging of the external capacitor and can be used with a power supply in the range of 5-15 volts making it useful in many analog circuits. The simple temperature-sensitive circuit oscillated LEDs at a frequency proportional to the temperature sensed by the thermistor. Although this circuit served as a useful demonstration of the SL/DW process, there were several issues identified that required improvement before extending to more complex circuitry. For example, improved methods were required to accurately register the DW system with the embedded electronic components during changeover and a method was required to remove or cure uncured resin in component cavities prior to and after component insertion. In addition, although the E1660 ink was previously selected as the conductive media based on a simple resistivity experiment, further testing was required to measure impedances that arise in the conductive media when designing more complex 3D circuits. The following sections include descriptions of several

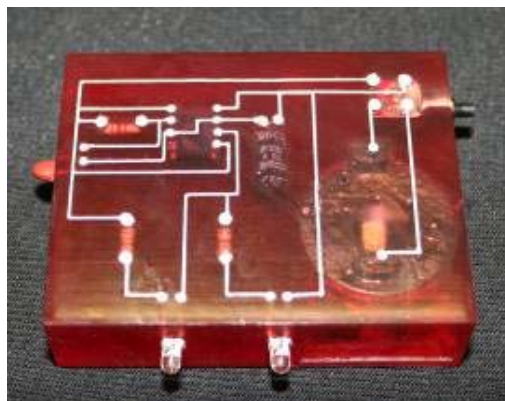


**Figure 1. LM555 temperature circuit fabricated using the hybrid SL/DW setup.**

improvements to the SL/DW process and the issues mentioned above with particular focus on applying this technology to a complex wireless motion sensor with navigation capabilities designed for a border security application.

### SL/DW Building Constraints

In order to successfully design and build a circuit for LM, several considerations were made. These LM constraints, however, do not alter the performance of the overall circuit in either PCB or 3D, although they do help to simplify the design process and to ease fabrication of a 3D circuit. First, the number of components was minimized in order to reduce the requirements for component embedding. Second, the DW process imposed a minimum pitch requirement on the components. Using the smallest dispensing tip available (6-mil inner diameter), a DW ink trace of 8-mil width was achieved consistently. Therefore, trace width was limited to ~8-mil and the pin pitch spacing of the electronic components had to be greater than 8-mil. Finally, with SL, low powered and low frequency electronic components were preferred in order to minimize heat dissipation requirements as a result of component embedding (obviously, creative strategies can be employed for thermal management, but we elected to minimize heat load to reduce complexity of the design in the preliminary design).

### Motion Sensor Design

Hardware components for the motion sensor system architecture were selected based on the SL/DW manufacturing constraints mentioned previously and included additional selection criteria based on compatibility and cost. The rPIC12F675K (Microchip Technology Inc., Chandler, Arizona) was selected as the microcontroller for the motion sensor due to its embedded RF circuitry and low power and cost. With the integration of RF circuitry in the microcontroller, components such as capacitors, inductors, filters and pre-amps were eliminated from the RF transmitter design. Although this integration proves useful during the 3D circuit design, other features were omitted from the microcontroller, which were useful in other areas such as Universal Synchronous Asynchronous Receiver Transmitter (USART). USART is needed for the rPIC12F675K to communicate to a PC serial port and GPS module, and, as a result, a software solution called ‘bit banging’ was implemented as will be described below. A Polstar PGM-101 (Polstar Technologies, Hsinchu City, Taiwan) was selected as the GPS module. PGM-101 measures 27 mm X 27 mm X 9 mm and consumes 120 mW via a 3.3VDC. Passive infrared (PIR) sensors were chosen as the motion sensor system due to the wide motion sensing area and small size that allows them to be easily embedded in SL. The Panasonic MP1211 (Panasonic Electric Works Corporation of America, New Providence, New Jersey) was selected and has a motion sensing area of 110° at a maximum distance of 10 meters and requires 5V charge and 0.17μA current during operation. A block diagram of the motion sensor is illustrated in Figure 2.

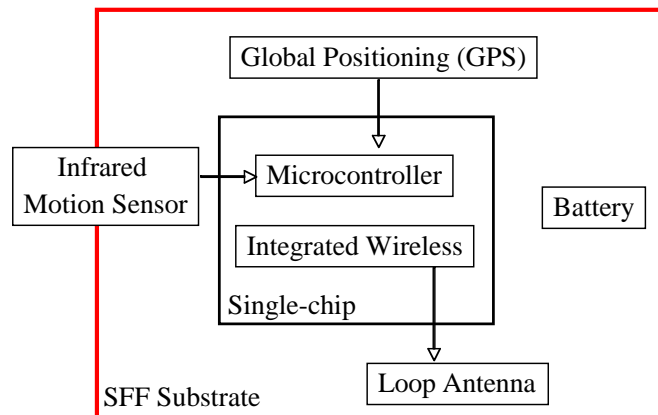


**Figure 2. Motion sensor block diagram.**

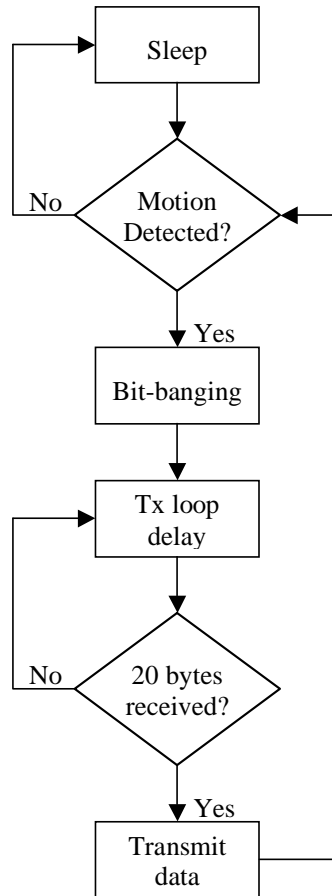


**Figure 3. Motion sensor operation software flowchart.**

A considerable challenge faced during the development of the motion detection system was in the software programmed in the rfPIC12F675K. Due to the lack of a USART interface in the rfPIC12F675K, a ‘bit-banging’ subroutine was written for the rfPIC12 using Assembly Language. ‘Bit-banging’ is a technique created for facilitating serial communications to use software instead of dedicated hardware such as a USART or shift register, which will allow the rfPIC12F675K to communicate and receive serial data from the GPS receiver. A ‘transmit’ code was also written to control the operating mode and to initialize the transmission loop and Tx buffer register once the ‘bit-banging’ subroutine was called. Assembly Language was used to write the complete software for the rfPIC12F675K and burned via In-Circuit-Serial-Programming technique. Figure 3 shows a flow chart of the motion sensor software operation.

The Motion Sensor is initially in sleep mode to consume the least amount of current to prolong battery life. When motion is detected by a difference in infrared radiation, the PIR sensor sends a ‘high signal’ of  $V_{DD}$  to the rfPIC12F675K microcontroller interrupting it from sleep mode and calls the bit-banging subroutine. 20 bytes of NMEA format GPS coordinates are then transmitted at 315 MHz. NMEA is a standard protocol used by GPS receivers to transmit data.

### **PCB Demonstration**

The software was debugged using MPLAB IDE v7.60 (Microchip Technology Inc., Chandler, Arizona) and voltages were measured at various points using a MeTex® multimeter

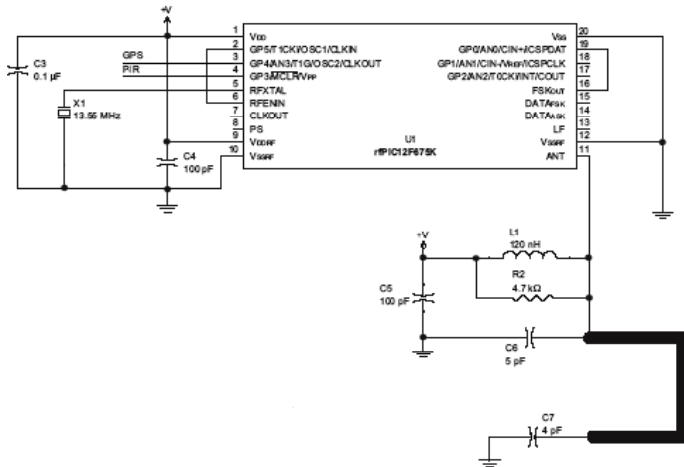


**Figure 4. Final motion sensor schematic.**

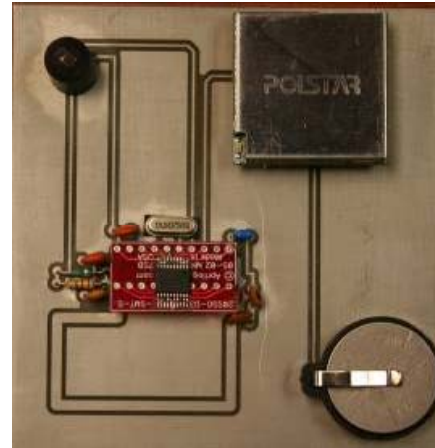


**Figure 5. PCB motion sensor.**

(Model # M-3850D) to validate the motion sensor design. Once all software and components were operating as expected, a final schematic of the motion sensor was created as shown in Figure 4 and a PCB board was created as shown in Figure 5.

Two MeTex® multimeters (Model # M-3850D) and a Tektronix oscilloscope (Model # TDS 210) were used to check proper voltages and signal output in order to test the operation and transmission of the motion sensor. The output voltage of the PIR sensor was measured to check for 'high-low' (VDD to GND) voltage transition when motion was detected. The voltage at the RFENIN (Radio Frequency Enable Input) pin was measured to check if the pin went high (GND to VDD) and enabled the RF transmitter and then whether the RFENIN pin went low after transmission, indicating that the rfPIC12F675K had changed to sleep mode disabling the transmitter. Oscilloscope probes were placed on ground and at the ANT (Antenna) pin of the rfPIC12F675K to check whether the RF transmission was valid. The sensor was placed on the floor in a hallway with students walking by to activate the motion sensor, and the 20-byte GPS RF transmission was measured with results shown in Figure 6 signifying that the motion sensor was operating as designed. When no motion was detected, the output signal had a DC voltage of 0V indicating that no signal was being transmitted.

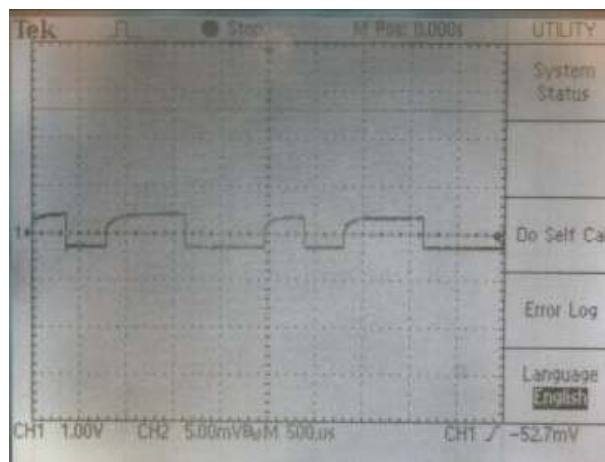


**Figure 6. Measured antenna output of PCB motion sensor using two probe oscilloscope.**

### DW Parasitic Test

Through the work of Lopes *et al.* (2006), the comparison of average resistivity of various inks on different substrates determined that E1660 silver conductive ink had the lowest average resistivity after thermal curing. This conclusion was valid for low-voltage direct current (DC) circuits because frequency and high voltages were not considered. The motion sensor has several outputs with alternating voltage, thus indicating that there is a frequency factor that needs to be considered when evaluating potential conductive media and their parasitic losses. The capacitance reactance is known as  $X_C$ , inductive reactance is known as  $X_L$  and each is described by Equation 1:

$$\text{(Equation 1)} \quad X_C = \frac{1}{2\pi * f * C} \quad X_L = 2\pi * f * L$$

Capacitance impedes a change in voltage while inductance impedes a change in current.  $X_C$  is large at low frequencies and small at high frequencies, and at DC,  $X_C$  is infinite. The opposite is true for  $X_L$ .  $X_L$  is small at low frequencies and large at high frequencies, and at DC,  $X_L$  is zero. Therefore, in an AC circuit, one cannot ignore the frequency effects. Every wire, trace, component, or material experiences these impedances, and whether these factors will significantly affect the performance of a circuit needs to be determined. To measure RLC values in various conductive media, SL parts with ink channels were designed using SolidWorks to obtain high RLC values. The SL images of the three RLC test models are shown in Figure 7. The E1660 (E1660-136, Ercon, Wareham, MA), E1440 (E1400-136, Ercon, Wareham, MA), PTF-10A (PTF-10A, Advanced Conductive Materials Inc., Atascadero, Calif.), and CI-1001 (CI-1001, ECM LLC, Delaware, OH) were four inks chosen for the RLC test (see Lopes *et al.*, 2006, for a discussion of these inks). The channel width for this experiment was 0.010" (small enough for the pitch we were considering) and the channel depth was 0.004". The designed parts were sliced using the 3D Lightyear™ software and manufactured on a standard SLA 250/50 stereolithography machine. The RLC samples were cleaned and cured using Isopropyl alcohol. Using a direct application method, the ink was evenly applied into the grooves by using a simple 'cotton Q-tip'. A paper sprayed with alcohol was used to remove excess ink from the surface, while the required ink remained in the channels. The samples were then placed in an oven at the manufacturer's recommended temperature for 10 minutes (cured samples shown in Figure 7).

Since small RLC values were expected, a high resolution Agilent LRC Meter (Model # 4262B, Santa Clara, CA) was used to measure the RLC values of the SL test models. After initializing the LCR Meter with our initial test parameters (1 kHz, 1000mV, 0 m cable length), a 4-point probe setup was used by connecting a Device Under Test (DUT) attachment. To calibrate the LCR meter, an open loop and closed loop test was preformed to eliminate any stray parasitic values that may be induced by the instrument and test probes on the test samples. The testing parameters  $R$ ,  $C_P$  and  $L_P$  were selected to be measured. Test probes were placed at the opposite ends of the ink traces on each test sample to measure the RLC values and repeated four times. Table I illustrates the average measured resistance, capacitance and inductance values with standard deviation, and these results are plotted in Figure 8. Table II shows the calculated average capacitive and inductive reactance values with standard deviation (using Equation 1) and these results are plotted in Figure 9.

To determine the optimal conductive ink for the wireless sensor application, all conductive ink parasitic measurements were compared to an equivalent PCB test model. E1660's parasitic values closest compared to the PCB model suggesting that the impedance values of E1660 will

have a minimal effect on the radiation of electromagnetic waves compared to the other conductive inks tested.

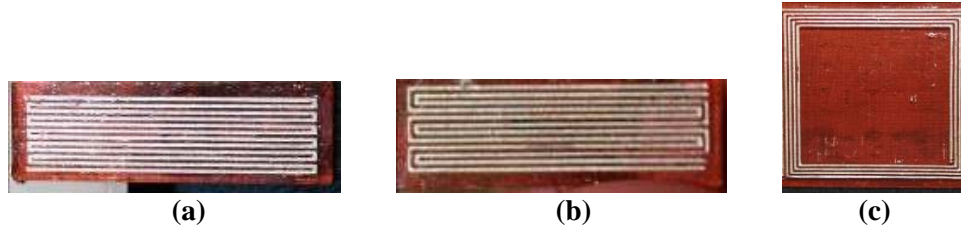
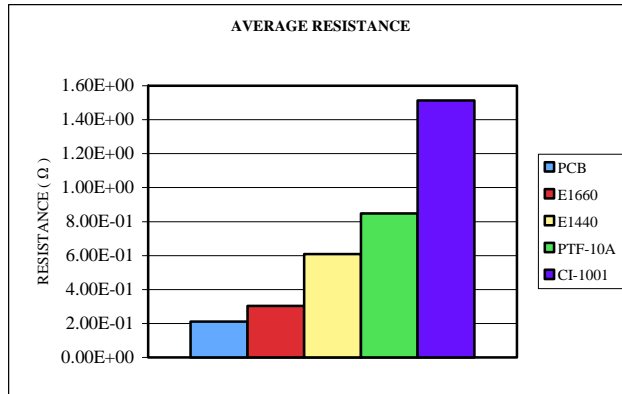


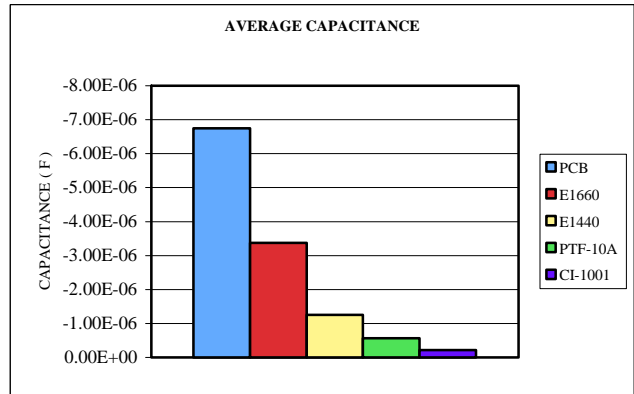
**Figure 7. Cured ink SL RLC test models; (a) Serpentine design increases resistance over length of ink line to allow for measurable data; (b) Parallel serpentine design increases capacitance over length of ink line to allow for measurable data; (c) Loop design allows for the inductance of two adjacent ink lines to add while minimizing the attenuation of their magnetic field.**

**Table I. Average and standard deviation of measured RLC values.**

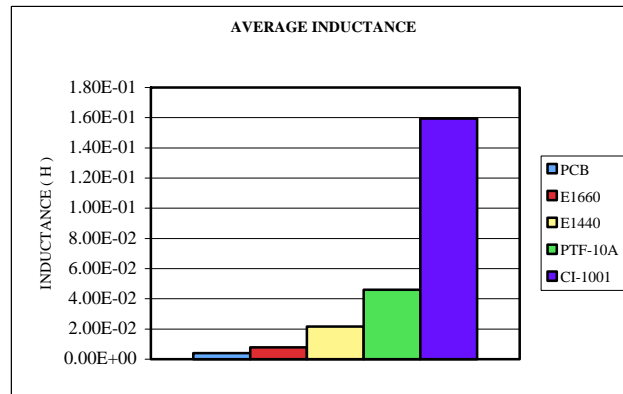
TEST SAMPLE	AVERAGE RESISTANCE ( $\Omega$ )	RESISTANCE STANDARD DEVIATION	AVERAGE CAPACITANCE (F)	CAPACITANCE STANDARD DEVIATION	AVERAGE INDUCTANCE (H)	INDUCTANCE STANDARD DEVIATION
PCB	2.117E-01	1.127E-02	6.750E-06	1.215E-06	3.978E-03	9.869E-04
E1660	3.039E-01	7.944E-03	3.375E-06	1.130E-06	7.775E-03	1.242E-03
E1440	6.094E-01	1.462E-01	1.253E-06	5.397E-07	2.165E-02	8.552E-03
PTF-10A	8.475E-01	1.221E-01	5.611E-07	7.465E-08	4.609E-02	1.768E-02
CI-1001	1.513E+00	8.382E-02	2.203E-07	1.371E-08	1.595E-01	1.887E-02



**(a)**



**(b)**

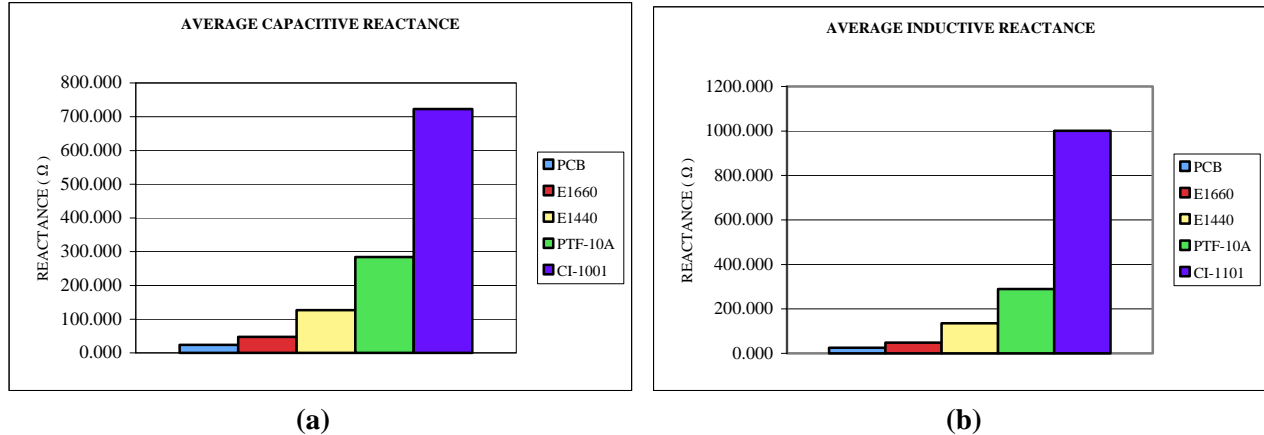


**(c)**

**Figure 8. Average measured RLC values of a PCB and four DW inks using an LCR meter; test was repeated four times (N=4): (a) Resistance; (b) Capacitance; (c) Inductance.**

**Table II. Average and std deviation of calculated capacitive and inductive reactance.**

TEST SAMPLE	CAPACITIVE REACTANCE ( $\Omega$ )	CAPACITIVE REACTANCE STD DEV	INDUCTIVE REACTANCE ( $\Omega$ )	INDUCTIVE REACTANCE STD DEV
PCB	23.590	4.533	24.979	6.198
E1660	47.181	21.864	48.827	7.800
E1440	127.035	51.974	135.962	53.707
PTF-10A	283.805	39.023	289.414	111.005
CI-1001	722.731	45.709	1001.503	118.487

**Figure 9. Average reactance of a PCB and four DW inks: (a) Capacitive Reactance (b) Inductive Reactance.**

### Design and Assembly for Layered Manufacturing

To design the motion sensor in 3D, the PCB schematic was considered as a model divided into several smaller integrated sections. Using SolidWorks software, each component was designed to be placed on the bottom surface of the motion sensor with four vias to secure each pin and to provide a better interface for the DW ink. Although one design solution would place each component adjacent to other components in order to reduce the area of the circuit, this is not practical for the loop antenna components. Since this section of components emits electromagnetic fields, the proximity and angle of each component is critical for proper transmission. Therefore, this section of components was transferred directly from the schematic (and thus, similar to the layout of the PCB). To allow access for the DW ink to the rfPIC12F675K's low profile pins, a fitted cavity was designed for the microcontroller to 'press fit' on the top surface of the sensor. Ink traces were drawn in the model to assist with measuring the position of each ink trace when registering for DW depositing. The body of the motion sensor was modeled after a rock with a cavity designed within it to embed the motion sensor. By creating multiple parts that snap together, components were packaged closer together, which resulted in smaller complex designs of arbitrary shape. The CAD models of the resulting motion sensor are shown in Figure 10.

The hybrid SL/DW setup was utilized to manufacture both the motion sensor and the rock body with DSM Somos® ProtoTherm<sup>TM</sup> resin and E1660 conductive ink. The SL/DW process was initiated by first fabricating the motion sensor with component vias in one continuous build. Once the SL part was built, it was removed from the SL/DW setup platform, and the cavity and component vias were cleaned using Isopropyl alcohol and cured in a UV oven prior to inserting the electronic components. The electrical components were manually placed on the bottom surface of the motion sensor. Each component pin was inserted upward through one via and then back through a second via and clipped using wire cutters. This process fixed the component in

place and created a snap fit for the pin. The rfPIC12F675K and its pins were aligned on the top surface with its cavity, and then press fitted into place. Figure 11 shows this process.

To dispense the DW ink, the position of each ink trace for the motion sensor was measured using the ink trace replica in the SolidWorks model. The measured coordinates were input in a LabVIEW® program which controls the DW traverse stages with the dispensing pump and syringe. The DW dispensing process is illustrated in Figure 12. To embed the motion sensor, the rock model was fabricated in the SL/DW setup with a build stop at a predetermined layer. The motion sensor with components and DW ink traces was placed into the cavity and the build was continued. Additional details of the DW dispensing process and the build stop procedure required to embed components are provided in Lopes *et al.* (2006).

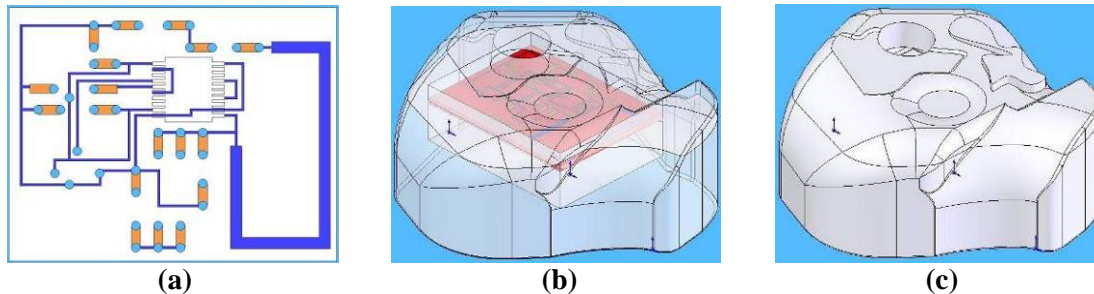


**Figure 10. SolidWorks motion sensor assembly design:** (a) Part I of the motion sensor design includes component vias shown in orange, ink trace replica shown in blue and the rfPIC12F675K cavity; (b) Part II of the motion sensor includes the body of the sensor, which is modeled after a rock and includes a cavity for the embedding of the sensor shown in red; (c) Complete assembly of the motion sensor.

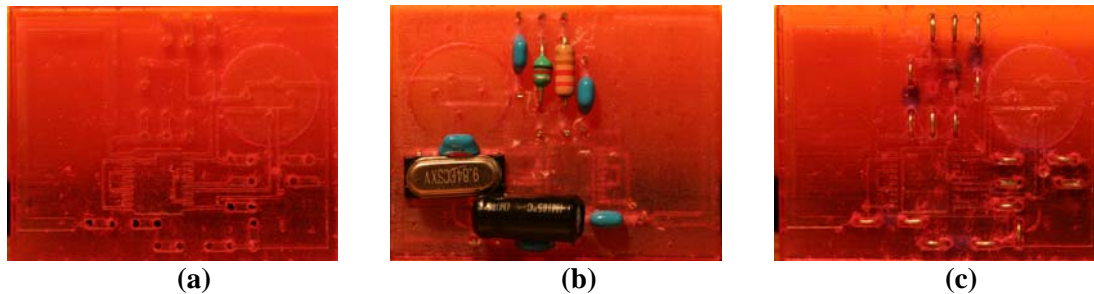


**Figure 11. Fabricated SL motion sensor:** (a) fabricated motion sensor with component vias, and cavity; (b) components placed at the bottom surface with pins inserted through vias; (c) top surface of the motion sensor with pins snap fitted in place.

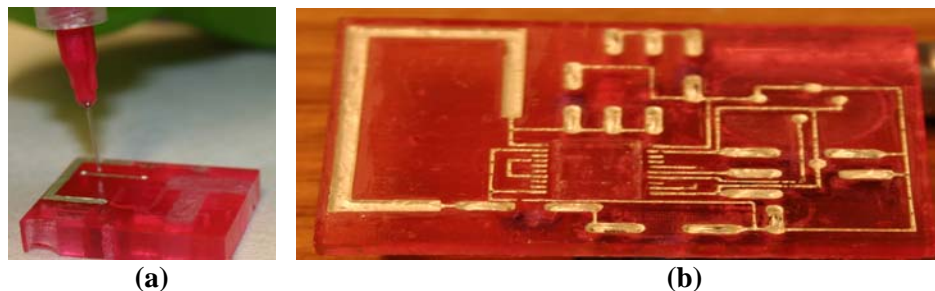


**Figure 12. DW ink dispensing process:** (a) DW traverse stage outlines and dispenses E1660 ink on the top surface of the motion sensor; (b) completed DW ink dispensing.

## Demonstration

The functional hybrid SL/DW part was compared to the PCB motion sensor for functionality. Since all components in the layer manufactured sensor were embedded, it was difficult to test voltages and output signals of the motion sensor using a multimeter and oscilloscopes without damaging the circuit. Therefore, to test the 3D motion sensor, a Graphical User Interface (GUI) and a receiver circuit were developed. The receiver setup collected any information transmitted from the sensor once motion was detected and converted the information to Recommended Standard 232 (RS232) format. The GUI application also displayed the GPS coordinates in NMEA format. To simulate this, a laptop with the GUI and receiver setup were placed 10 meters from the motion sensor outside in an open field. As a person walked past the motion sensor, movement was successfully detected and the GPS data were displayed on the GUI application as shown in Figure 13.

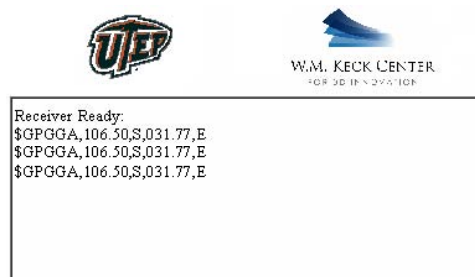


**Figure 13. 20 bytes of GPS data received after the motion sensor was triggered and displayed via a GUI application.**

## Conclusion

A wireless motion sensor with GPS navigation was designed based on functional requirements and SL/DW building constraints. A PCB version of the motion sensor was fabricated and tested in order to test the operation of the motion sensor. A 3D model was proposed to incorporate the functional requirements of the motion sensor. In order to achieve accurate transmission of information in complex circuitry (with fluctuating voltages and currents), a suitable conductive media for DW with parasitic values comparable to copper traces was desired. An RLC test was performed using SL parts designed to obtain high parasitic values. Four DW inks were dispensed using a direct application method and cured at the recommended curing conditions. An LCR Meter was used to measure resistance, capacitance, and inductance at 1 kHz frequency and reactance was calculated using standard capacitive and inductive reactance equations. Based on these tests, E1660 from Ercon Inc., Wareham, MA was found to have the most comparable RLC values to copper traces and was chosen as the DW ink. To fabricate the sensor, an assembly of parts was designed using SolidWorks in order to achieve the most compact design suitable for fabricating a 3D motion sensor using layered manufacturing. A hybrid SL/DW machine was used for manufacturing embedded electronic components in a semi-automated environment with DW interconnects. A GUI and a receiver circuit were designed to test the performance of the 3D motion sensor and both the PCB and 3D circuits showed similar performance.

## Future Work

There are further important parameters that affect the performance of DW ink antenna that need to be investigated. Attenuation, phase, bandwidth and the resonant frequency need to be measured in order to better tune the antenna and to improve the design of future wireless applications. SL properties need to be evaluated in extreme temperature such as prolonged exposure to heat, cold and UV. These evaluations will assist in the overall 3D design of the application in order to accommodate these conditions.

### Acknowledgments

The facilities within the W.M. Keck Center for 3D Innovation (Keck Center) used here contain equipment purchased through Grant Number 11804 from the W.M. Keck Foundation, a faculty STARS Award from the University of Texas System, and two equipment grants from Sandia National Laboratories. This material is based in part upon work supported through the Mr. and Mrs. MacIntosh Murchison Chair I in Engineering and through research contract 504004 from Sandia National Laboratories in the Laboratory Directed Research and Development (LDRD) program. Sandia National Laboratories is a multi-program laboratory operated by Sandia Corporation, a Lockheed Martin Company, for the United States Department of Energy's National Nuclear Security Administration under contract DE-AC04-94AL85000.

### References

1. A.J. Lopes, M. Navarrete, F. Medina, J.A. Palmer, E. MacDonald, R.B. Wicker, "Expanding Rapid Prototyping for Electronic Systems Integration of Arbitrary Form", *Proceedings of the 2006 Solid Freeform Fabrication*, Austin, Texas, 2006.
2. D. Begaye, "Optical Transmission on Digital Signals through Rapid Prototyping Fibers", 2003 National Conference on Undergraduate research, Salt Lake City, Utah.
3. DSM Somos, June 2002, *ProtoTherm 12120 –Product Data Sheet*, New Castle: Delaware, [www.dsmsomos.com](http://www.dsmsomos.com), 03/27/2005.
4. ECM LLC, 2004, *CI-1002 – Product Data Sheet*, Delaware, Ohio, [www.conductives.com](http://www.conductives.com), 06/15/2005.
5. F. Medina, A.J. Lopes, A.V. Inamdar, R. Hennessey, J.A. Palmer, B.D. Chavez, and R.B. Wicker, "Integrating Multiple Rapid Manufacturing Technologies for Developing Advanced Customized Functional Devices," *Rapid Prototyping & Manufacturing 2005 Conference Proceedings*, Rapid Prototyping Association of the Society of Manufacturing Engineers, May 10-12, 2005a, Hyatt Regency Dearborn, Michigan.
6. F. Medina, A.J. Lopes, A.V. Inamdar, R. Hennessey, J.A. Palmer, B.D. Chavez, D. Davis, P. Gallegos, and R.B. Wicker, "Hybrid Manufacturing: Integrating Direct-Write and Stereolithography", *Proceedings of the 2005 Solid Freeform Fabrication*, Austin, Texas, 2005b.
7. R. Mosses; S. Brackenridge, "A Novel Process for the Manufacturing of Advanced Interconnects", *Circuit World*, Volume 29, Number 3, 2003, pages 18-21.
8. T. F. L. Ocampo, "Incorporation of Electrical Components into Rapid Prototyped Products", 2003 National Conference on Undergraduate Research, Salt Lake City, Utah.
9. J.A. Palmer, P. Yang, D.W. Davis, B.D. Chavez, P.L. Gallegos, R.B. Wicker, and F.R. Medina, "Rapid Prototyping of High Density Circuitry," *Rapid Prototyping & Manufacturing 2004 Conference Proceedings*, Rapid Prototyping Association of the Society of Manufacturing Engineers, May 10-13, 2004, Hyatt Regency Dearborn, Michigan. Also, *SME Technical Paper TP04PUB221* (Dearborn, Michigan: Society of Manufacturing Engineers, 2004).
10. J.A. Palmer, J.L. Summers, D.W. Davis, P.L. Gallegos, B.D. Chavez, P. Yang, F. Medina, and R.B. Wicker, "Realizing 3-D Interconnected Direct Write Electronics within Smart Stereolithography Structures," *International Mechanical Engineering Congress and Exposition 2005 Proceedings*, November 14-18, 2005, Orlando, Florida.